

MASTER

CONF-790219--10

March 1979

**Neutron Scattering Studies of Pretransitional Phenomena
in Structural Phase Transformations**

S. M. Shapiro

The submitted manuscript has been authored under contract EY-76-C-02-0016 with the Division of Basic Energy Sciences, U.S. Department of Energy. Accordingly, the U.S. Government retains a nonexclusive, royalty-free license to publish or reproduce the published form of this contribution, or allow others to do so, for U.S. Government purposes.

NOTICE

This report was prepared as an account of work sponsored by the United States Government. Neither the United States nor the United States Department of Energy, nor any of their employees, nor any of their contractors, subcontractors, or their employees, makes any warranty, express or implied, or assumes any legal liability or responsibility for the accuracy, completeness or usefulness of any information, apparatus, product or process disclosed, or represents that its use would not infringe privately owned rights.

DISTRIBUTION OF THIS DOCUMENT IS UNLIMITED
WDM

Neutron Scattering Studies of Pretransitional Phenomena
in Structural Phase Transformations

S. M. Shapiro

Brookhaven National Laboratory, Upton, New York 11973

DISTRIBUTION OF THIS DOCUMENT IS UNLIMITED

Materials exhibiting structural phase transformations are well known to possess pretransitional phenomena. Below the transition temperature, T_c , an order parameter appears and the pretransitional effects are associated with the fluctuations of the order parameter. Neutron scattering techniques have proved invaluable in studying the temporal and spatial dependence of these fluctuations. SrTiO_3 is the prototypical example of a structural phase transformation exhibiting features observable in other transformations such as martensitic and order-disorder. The experimental evolution of the understanding of the phase transformation in SrTiO_3 will be reviewed and the features observed will be shown to typify other systems.

I. INTRODUCTION

Landau Theory

In this discourse I shall review the role neutron scattering has played in the understanding of structural phase transformations. The experimental understanding of these transformations will be traced by discussing in detail the transformation in the insulating compound SrTiO_3 , which can be considered as a prototypical system. Other metallic systems will then be discussed and shown to exhibit features similar to those observed in SrTiO_3 .

Let us begin with a brief review of the Landau theory of phase transitions¹ and show how, qualitatively at least, it describes many of the features observed in a phase transformation.

Consider the expansion of the free energy of the system in terms of an order parameter, η :

$$F - F_0 = \frac{1}{2} a(T)\eta^2 + \frac{1}{4} b\eta^4 + \frac{1}{6} c\eta^6 + \dots \quad (1)$$

Since highly symmetric systems will be considered, only even powers of η are included. The coefficients b and c are assumed to be temperature independent and $a(T)$ has the form

$$a(T) = a_0(T - T_c) \quad (2)$$

It is through this temperature dependence that the pretransitional phenomena are revealed. The sign of b determines the nature of the

transition. If $b > 0$, the transition is second order and continuous; if $b < 0$, it is first order, and if $b = 0$, there is a tricritical point where a line of first order transitions meets a line of second order transitions.

Let us consider the transition to be second order and deal only with the first two terms of Eq. (1). Applying the equilibrium conditions $\partial F/\partial \eta = 0$ and $\partial^2 F/\partial \eta^2 > 0$ we obtain for equilibrium values of η :

$$\begin{aligned} &= 0 && T > T_c \\ \langle \eta \rangle &= \pm \sqrt{\frac{a_0 (T_c - T)}{b}} && T < T_c \end{aligned} \quad (3)$$

Thus the average value of the order parameter is 0 above T_c and follows the power law $\langle \eta \rangle \sim (T_c - T)^\beta$ with $\beta = 1/2$ below T_c .

The physical nature of the order parameter depends, of course, on the system being studied. In magnetic systems and ferroelectricity, it is the spontaneous magnetization and polarization, respectively. In order-disorder systems, it might represent an occupation of a particular site in the lattice. In structural transformations, it corresponds to displacements of atoms from some highly symmetric position.

Much can be learned from looking at a graph of the free energy at different temperatures. Fig. 1 shows a plot of Eq. (1) for $T > T_c$, $T = T_c$ and $T < T_c$. At high temperatures, the quadratic term dominates for small η and the energy has an approximate parabolic shape with a

minimum at $\langle \eta \rangle = 0$. However, fluctuations can occur about this minimum and the size of these fluctuations corresponds to the shape of the well about $\langle \eta \rangle = 0$. As $T \rightarrow T_c$, $a(T) \rightarrow 0$ and the well becomes flatter near $\eta = 0$ and consequently the fluctuations increase. These critical fluctuations or pretransitional phenomena can become very large near T_c . Finally, below T_c because of the negative sign of $a(T)$, minima develop for finite values of η which are the new equilibrium values of the order parameter.

These potential curves also provide insight into the dynamical behavior one would expect. This results from the fact that $\partial^2 F / \partial \eta^2$, which is a measure of the curvature of the well, is also proportional to a thermodynamic frequency ω_0^2 . From Eq. (1) we see

$$\omega_0^2 \equiv a_0 (T - T_c) \quad . \quad (4)$$

As $T \rightarrow T_c$ from above, the frequency of a particular mode of the system will decrease towards zero. This soft mode concept was developed about 20 years ago.² The first observation of a soft mode was made almost 40 years ago in crystalline quartz,³ although the connection between the change in frequency and the phase transition was not clear at that time. The ideas have been refined extensively since then.⁴

The displacements associated with this particular mode, ω_0 , are precisely those necessary to bring the system from one symmetry phase to another. At T_c , these displacements can be viewed as being frozen, corresponding to $\omega_0 = 0$.⁵

NEUTRON SCATTERING

Before discussing particular systems, it will be useful to describe the techniques of neutron scattering and compare with x-ray scattering. In thermal neutron scattering, the wavelength of the neutron lies between $\lambda \sim 1$ to 5 \AA with energy $E \sim 3$ to 100 meV ($1 \text{ meV} \equiv 8.07 \text{ cm}^{-1} \equiv 11.6 \text{ K} \equiv 0.24 \text{ THz}$). These values are on the same order as the atomic separations and the lattice energies in a solid. Thus neutrons allow not only the measurements of atomic positions in a solid, as do x-rays, but also the vibrational motion of the atoms. This is accomplished by energy analysis of the scattered neutrons.

At Brookhaven National Laboratory, inelastic measurements are performed at the 40MW High Flux Beam Reactor whose maximum thermal neutron flux is 0.7×10^{15} neutrons/cm²-sec. A triple-axis spectrometer is used and shown schematically in Fig. 2. A single energy is selected from the reactor spectrum by a monochromator crystal. The sample sits at the second axis position. The neutrons scattered by the sample are energy analyzed via Bragg's law from the third crystal and then detected by a BF_3 detector.

The scattered intensity is proportional to the dynamical structure factor $S(\vec{Q}, \omega)$ where $\vec{Q} = \vec{k}_i - \vec{k}_f$ and $\hbar\omega = \frac{\hbar^2}{2m} (k_i^2 - k_f^2)$ represent momentum and energy conservation:

$$I(\vec{Q}, \omega) \sim \frac{k_f}{k_i} S(\vec{Q}, \omega) \quad (5)$$

where k_i and k_f are the initial and final wave vectors of the neutron.

$S(\vec{Q}, \omega)$ contains the physics of interest and can be written, using the fluctuation dissipation theorem:⁶

$$S(\vec{Q}, \omega) = (n(\omega) + 1) \text{Im}\chi(\vec{Q}, \omega) \quad (6)$$

where $\chi(\vec{Q}, \omega)$ is the Q dependent dynamical susceptibility. $(n(\omega) + 1)$ is the familiar Bose Einstein occupation number which for $kT \gg \hbar\omega$, $(n(\omega) + 1) = \frac{kT}{\hbar\omega}$. Since we are dealing with phonons in a solid, $\text{Im}\chi(\vec{Q}, \omega)$ has the form of a damped harmonic oscillator⁶

$$\text{Im}\chi(\vec{Q}, \omega) = \frac{\omega\Gamma_0}{(\omega_0^2(\vec{Q}) - \omega^2) + (\omega\Gamma_0)^2} \quad (7)$$

Γ_0 is proportional to the inverse of the lifetime of the phonon and related to the anharmonicity of the lattice.

Integrating Eq. (6) over energy and using Eq. (7)

$$S(\vec{Q}) = \int S(\vec{Q}, \omega) d\omega \sim \frac{T}{\omega_0^2(\vec{Q})} \quad (8)$$

Because of the large energy of x-rays ($\sim \text{keV}$) the integration in Eq. (8) is performed automatically. If there are modes with low frequencies, or a very anisotropic dispersion curve, streaks in the diffraction pattern associated with these low modes will appear. These are the rel rods so frequently observed. Inelastic neutron scattering allows one to establish whether these streaks or rods are dynamical or static in origin.

SrTiO_3

One of the most extensively studied systems exhibiting a structural phase transformation is SrTiO_3 . Fig. 3 shows a view of the structure as seen looking down a cubic axis. The Ti atoms are situated at the center of an octahedron of oxygen atoms. As the temperature is lowered towards 100 K, a transformation occurs from the high temperature cubic perovskite structure to a tetragonal symmetry. The tetragonal structure arises due to a rigid rotation of the oxygen octahedra by an angle ϕ about the three cubic axis.⁷ The mode associated with this rotation is also illustrated in Fig. 3. It clearly shows that the wavelength of this mode is twice the size of the unit cell. Since there is a rotation about the three cube axis, the wavelength of this mode corresponds to the $\vec{q}_R = (\frac{1}{2}, \frac{1}{2}, \frac{1}{2})$ point in reciprocal space. Following the qualitative arguments discussed above, as $T \rightarrow T_c$, the frequency of this mode should decrease and eventually a Bragg peak should appear at the $(\frac{1}{2}, \frac{1}{2}, \frac{1}{2})$ point when the mode frequency becomes zero. This was first confirmed by the inelastic neutron studies of Shirane and Yamada⁸ and their temperature dependent spectra are shown in Fig. 4. In Fig. 5, the temperature dependence of the soft mode frequency is seen to follow the prediction of Eq. (4) very well in that the solid line is a fit to the expression:

$$1/\hbar\omega_0^2 = a + \frac{c}{T - T_c}$$

with $T_c = 108\text{K}$, $a = 0.0081 \text{ meV}^{-2}$ and $c = 4.22 \text{ meV}^{-2}$. Since these experiments, many other structural phase transitions have been studied

and show a similar behavior.⁹

All seemed well for a short time, then experiments began to suggest that the simple Landau theory might not be quantitatively correct. Müller and Berlinger¹⁰ performed a careful measurement of the order parameter below T_c by EPR measurements and claimed $\eta \sim (T_c - T)^\beta$ with $\beta = 0.33$, not $\beta = \frac{1}{2}$ as predicted by the Landau theory. In addition, Riste et al¹¹ and Shapiro et al¹² observed a strong diverging "central component," centered at $\hbar\omega = 0$ and at the q_R point whose intensity diverged as T_c was approached from above.

Fig. 6 shows energy scans at the q_R point for several temperatures near T_c . The phonon is seen to soften but as seen on the right side, there is a clear divergence in intensity at $\hbar\omega = 0$. This central peak-soft mode behavior has now been observed in many systems by neutron¹³ and light scattering techniques.¹⁴ In fact, the divergent central peak has now become the rule, not the exception, in most structural phase transformations.

What is its origin? Cowley¹⁵ proposed that the central peak has a dynamical origin related to the anharmonicity in the crystal. Simply put, the soft phonon can decay into some thermal phonons. This is the origin of the line width Γ_0 of Eq. (7). These thermal phonons then have a lifetime τ of their own and also decay. This has the mathematical effect of introducing a frequency dependent damping into the term Γ_0 .¹² On this basis, one would expect the central peak to have a line width comparable to that of phonons in a solid, i.e. a width $\tau^{-1} \sim 1 - 2$ meV. However, extremely high resolution neutron scattering studies have been able only to put an upper limit to the line width¹⁶

of $\tau^{-1} < 0.08 \mu\text{eV}$ ($\sim 20\text{MHz}$).

Because no energy line width of the central peak has been observed, a static mechanism which is defect induced, seems more likely. This was first suggested by Axe and Shirane.¹⁷ Defects in a lattice will generally give rise to displacements of neighboring atoms from their equilibrium positions. These displacements cause the diffuse scattering known as Huang scattering. The magnitude of the displacement field can be calculated as a linear response to a force field F which the impurity exerts on the undisplaced atoms. The amplitude of the displacement can be written in terms of phonon modes

$$\langle Q_j \rangle = F_j / \omega_j^2$$

where j represents a particular mode and ω_j the frequency of that mode. The observed intensity of this static diffuse scattering is then:

$$I_j(Q) \Big|_{\text{static}} \propto |\langle Q_j \rangle|^2 = \frac{|F_j|^2}{\omega_j^4}$$

If there is a soft mode in the system $\omega_j^2 = \omega_0^2 \propto (T - T_c)$, then the elastic intensity will increase more rapidly since the intensity due to the condensing phonons goes only as $1/\omega_0^2$. This idea, which qualitatively at least conforms to the experiments, has been extended by other people and even allows for an energy line width due to a fluctuating defects.¹⁸

Experimental evidence of the involvement of a defect mechanism in the central peak formation was demonstrated recently in the study of the central peak in hydrogen reduced SrTiO_3 .¹⁹ When SrTiO_3 is reduced in a hydrogen atmosphere it becomes conducting with a relatively large number of free carriers ($n_c \sim 10^{20}/\text{cm}^3$). Several samples were available whose carrier concentration had previously been determined. T_c was found to decrease with carrier concentration and the central peak intensity was found to increase with n_c . Fig. 7 shows the intensity of the central peak as a function of $(T - T_c)$ for several samples, including a nominally pure sample. It is clearly seen that there is a systematic increase in the intensity of the central peak as the number of carriers increases. The carrier concentration is closely comparable to the defect concentration, but insufficient data exists to establish a functional relationship between the carrier concentration and the type and number of defects. Nonetheless, the central peak is shown to be enhanced by defects, but at this stage we cannot state that defects are the sole cause of the divergent central peak.

METALLIC SYSTEMS

We have demonstrated that in a structural phase transformation, a mode whose frequency decreases as T_c is approached contains the displacements necessary to go from the high to low temperature phase. These dynamical displacements are frozen out resulting in the low temperature structure. Associated in some way through a dynamical or static coupling is a central peak which diverges as the transition

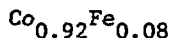
temperature is approached. Let us now look at some metallic systems and see how these pretransitional phenomena manifest themselves.

Nb_3Sn

Nb_3Sn is a familiar A15- β tungsten compound which is a high temperature superconductor with $T_c = 18.0$ K. At about twice this temperature, a martensitic phase transformation occurs at $T_M \approx 45$ K. This transition corresponds to a change of symmetry from cubic to tetragonal. Ultrasonic measurements have shown that the velocity of a shear wave corresponding to the elastic constants $(C_{11} - C_{12})/2$ practically vanishes at T_M .²⁰ Neutron scattering studies have extended the measurements to larger momentum transfers.^{17,21} All acoustic modes show a substantial reduction (10%) in frequency on cooling to T_M from 300 K, but the softening of the $[110]-T_1$ mode corresponding to $C_{11} - C_{12}$ is most pronounced. Fig. 8 shows the temperature dependence of the $[110]-T_1$ dispersion curve. The most drastic softening is observed for small q values. This can be considered as the soft mode of the system although there may be coupling to an optic mode or to some electronic excitation. In fact, it has been suggested that the kink appearing at the lower temperatures may be understood as a Kohn anomaly¹⁷ arising from the strong electron phonon interactions. The wave vector of the kink would then be connected with a dimension of the Fermi surface.

The neutron spectra are shown in Fig. 9. Note that the intensity scale is logarithmic. At 80 K, only the phonon is observed at $\hbar\omega = 0.4$ meV. As the transition temperature is approached, the phonon decreases in

energy and intensity begins to appear about $\hbar\omega = 0$. Finally, as one gets nearer to T_c , the central peak becomes the dominant feature of the spectra, with the phonon only visible as a shoulder. No energy line width was observable, but by a careful measurement of the intensity of the central peak it was concluded that the dynamical mechanism outlined above is primarily responsible for the central peak in Nb_3Sn .¹⁷



Pure cobalt undergoes a martensitic phase transition from a high temperature face-centered cubic (fcc) structure to a hexagonal closed pack (hcp) structure at $T_M \sim 420^\circ\text{C}$. Recent MÜssbauer measurements on a Co-7-wt%-Fe sample showed a decrease in T_M to $\sim 140^\circ\text{C}$ and an anomalous decrease of Debye-Waller factor at the phase transition²² which was interpreted as an increase in the root mean-square displacement of the atoms due to a change in interatomic force constants. This suggests that some form of lattice softening takes place which characterizes the transition from fcc to hcp. The modes contributing to the softening can be seen with the aid of Fig. 10.²³ This shows the stacking of the (111) planes of the fcc structure with sequence ABC ABC ABC. In transforming to the hcp phase the stacking becomes AB AB AB. This transformation is accomplished as shown in Fig. 10 by the displacements of two waves of wavelengths $6d_{(111)}$ and $3d_{(111)}$ where $d_{(111)}$ is the (111) interplanar spacing. The amplitudes of these waves are related by $\sqrt{3}$ to give precisely the hcp stacking. Both waves are propagating along [111] with polarization along the $[\bar{1}1\bar{2}]$ direction. The actual displacements required however are large ($\sim 0.41 a_0$ where $a_0 = 3.56 \text{ \AA}$

is the cubic lattice parameter) as the close-packed planes have to roll over each other past a potential barrier caused by the bridge between close-packed atoms in the planes. The transformation is therefore first order both because of the large displacements and because of the above barrier.

Inelastic neutron scattering experiments were performed on a sample of $\text{Co}_{0.92}\text{Fe}_{0.08}$ to search for the mode softening at the q vector predicted in Fig. 10. For this choice of Fe concentration, the cubic phase is stable at room temperature and, unfortunately, T_M probably occurs below 0 K. Thus, no transition was observed.

The Mössbauer results are surprising and we are led to suspect that their composition might be substantially lower in Fe concentration.

A more appropriate system to look for these effects is solid helium which also exhibits an fcc-hcp phase transition under pressure. At a pressure of 5 kbars. helium freezes into an fcc structure and at $T = 40$ K and undergoes a transition to the hcp phase at $T = 18$ K. Because of the light mass and large zero point motion of He, pretransitional effects might be more clearly observable. Experiments are now planned to study this transition in solid He.

TiNi(Fe)

TiNi is an intermetallic compound which undergoes a martensitic phase transformation at $T_M \approx 300$ K. Resistivity and structural studies have shown that pretransitional phenomena are observed at temperatures well above T_M .²⁴ Recently, it was shown that by adding up to 3% for Ni, T_M is strongly suppressed and a premartensitic phase transformation occurs at T_0 .²⁵

Neutron scattering studies were performed on a single crystal of $\text{Ti}_{50.1}\text{Ni}_{46.7}\text{Fe}_{3.2}$.²⁶ For this composition T_M is shifted to below 80 K. Superlattice peaks were observed below $T = 231$ K slightly displaced from $(h/3, k/3, 0)$. The peaks are stronger with $h \neq k$ indicating that the distortion giving rise to the superlattice is phonon-like and transverse to the $[110]$ direction. Fig. 11 shows the scans about $(2/3, 1/3, 0)$ at three temperatures below T_0 .²⁷ At $T = 228$ K, the peak is clearly shifted from the commensurate, $(2/3, 1/3, 0)$ position but as T is lowered, the peak shifts toward the commensurate value. These incommensurate peaks appearing below T_0 are similar to the charge density waves (CDW) observed in layered compounds.²⁸ At about 225 K, there is a lock-in where commensurability is established.

Associated with the appearance of the CDW is an apparent rhombohedral distortion as shown in Fig. 12. These scans were performed on a polycrystalline sample of $\text{Ti}_{50}\text{Ni}_{47}\text{Fe}_3$. The splitting of the (110) and (111) Bragg peak, with little or no change in (100) is very suggestive of a rhombohedral distortion. However, the size of splittings is not exactly what is expected from a purely

rhombohedral distortion and the true symmetry must be more complicated.

Only very preliminary inelastic measurements have been performed. No soft mode has yet been observed which is associated with the appearance of the CDW, or the rhombohedral distortions. Only phonons near the zone center have been measured and as one approaches the $(2/3, 1/3, 0)$ point in reciprocal space only a broad quasielastic peak is observed. The "soft mode" in this problem has yet to be located.

SUMMARY

In this brief review, I have tried to demonstrate how neutron scattering has proven invaluable in the study of pretransitional phenomena in structural phase transitions. SrTiO_3 is typical of many structural phase transitions in that a soft mode is seen to "freeze out" and a central peak diverges at T_c . Similar phenomena are observed in martensitic phase transitions in metals and a prediction of a soft mode was made for the fcc-hcp phase transformation. In the classic TiNi-Fe system, apparently a "little bit of everything" is occurring and the results presented are still preliminary.

ACKNOWLEDGMENTS

Much of the work presented here is a result of a fruitful and enjoyable collaboration with colleagues and visitors at Brookhaven National Laboratory. Research for this paper was supported by the Division of Basic Energy Sciences, Department of Energy, under Contract No. EY-76-C-02-0016.

REFERENCES

1. L. D. Landau, E. M. Lifshitz, Statistical Physics, p. 430, Pergamon, London, 1958.
2. P.W. Anderson, Fizika Dielektrikov (G. F. Skanavi, ed.) p. 290, Acad. Nauk USSR, Moscow, 1960; W. Cochran, Adv. Phys. 1960, Vol. 9, 1960, pp. 387-423; 1961, Vol. 10, pp. 401-411.
3. C. V. Raman, T. M. K. Nedungadi, Nature, 1940, Vol. 145, p. 147.
4. See papers in Structural Phase Transitions and Soft Modes, Ed. by E. J. Samuelsen and J. Feder, Universitetsforlaget, Oslo, 1971.
5. J. D. Axe and G. Shirane, Physics Today, 1973, Vol. 26, pp. 32-38.
6. S. W. Lovesey in Dynamics of Solids and Liquids by Neutron Scattering, Ed. S. W. Lovesey and T. Springer, Chapter I, Springer-Verlag, New York, 1977.
7. This was first recognized by P. A. Fleury, J. F. Scott, and J. M. Worlock, Phys. Rev. Lett. , 1968, Vol. 21, pp. 16-19.
8. G. Shirane and Y. Yamada, Phys. Rev. , 1968, Vol. 177, pp. 858-863.
9. G. Shirane, Rev. Mod. Phys. 1974, Vol. 46, pp. 437-439 ; Ref. 6, Chapter 2.
10. K. A. Müller and W. Berlinger, Phys. Rev. Lett. 1971, Vol. 26, pp. 13-16.
11. T. Riste, E. J. Samuelsen, K. Otnes, and J. Feder, Solid State Commun. 1971, Vol. 9, pp. 1455-1458,
12. S. M. Shapiro, J. D. Axe, G. Shirane, and T. Riste, Phys. Rev. 1972, Vol. B 6, pp. 4332-4341.
13. R. A. Cowley in Lattice Dynamics, Ed. M. Balkanski, p. 625, Flammarion, Paris, 1978.

14. P. A. Fleury and K. B. Lyons, *ibid*, p. 731; M. D. Mermelstein and H. Z. Cummins, *ibid*, p. 735.
15. R. A. Cowley, *J. Phys. Soc. Japan*, 1970, Vol. 28 suppl. pp. S239-241.
R. A. Cowley and G. J. Coombs, *J. Phys.*, 1973, Vol. C6, pp. 121-142, 143-157.
16. J. Töpler, B. Alefeld, and A. Heidemann, 1977, Vol. C 10, pp. 635-643.
17. J. D. Axe and G. Shirane, *Phys. Rev.* 1973, Vol. B8, pp. 1965-1977.
18. B. I. Halperin and C. M. Varma, *Phys. Rev.*, 1976, Vol. B9, pp. 4030-4044.
19. J. B. Hastings, S. M. Shapiro, and B. C. Frazer, *Phys. Rev. Lett.* 1978, Vol. 40, pp. 237-239.
20. K. R. Keller and J. J. Hanak, *Phys. Rev.* 1967, Vol. 154, pp. 628-632; R. Rehwald, *Phys. Lett.* 1968, Vol. 27A, pp. 287-288.
21. G. Shirane and J. D. Axe, *Phys. Rev. Lett.* 1971, Vol. 27, pp. 1803-1806.
22. B. B. Bokshtein, Y. B. Voitkovskii, G. S. Nikolskii, and I. M. Razumovskii, *Sov. Phys. JETP*, 1973, Vol. 37, pp. 283-286.
23. S. M. Shapiro and S. C. Moss, *Phys. Rev.* 1977, Vol. B15, pp. 2726-2730.
24. G. D. Sandrock, A. J. Perkins, and R. F. Hehemann, *Met. Trans.* 1971, Vol. 2, pp. 2769-2780.
25. M. Matsumoto and T. Honma, *Trans. Japan Inst. Metals*, 1976, Vol. 17 suppl, pp. 199-204.
26. M. B. Salamon, M. Meichle, C. M. Wayman, C. M. Huang, and S. M. Shapiro, *in press (AIP Series)*.
27. M. B. Salamon, S. M. Shapiro, and M. Meichle, unpublished, research done at Brookhaven National Laboratory.

28. D. E. Moncton, J. D. Axe, and F. J. DiSalvo, Phys. Rev. 1977,
Vol. B 16, pp. 801-819.

FIGURE CAPTIONS

- Fig. 1. Plot of the free energy function (Eq. (1)) for three different temperatures.
- Fig. 2. Schematic of a triple-axis spectrometer used at the HFBR of Brookhaven National Laboratory.
- Fig. 3. Crystal structure of SrTiO_3 as viewed looking down a cube axis. Top: the cubic phase; the arrows show the displacements of the atoms for the soft mode. Bottom: the tetragonal phase. The order parameter ϕ is the angle of rotation of the oxygen octahedra.
- Fig. 4. Inelastic spectra of SrTiO_3 for $T > T_c$ showing the decrease in frequency of the soft mode. The intensity at $\hbar\omega = 0$ near T_c was thought to be due to incoherent scattering and higher order contamination (from Ref. 8).
- Fig. 5. Top: the intensity of the new Bragg peak appearing below T_c . Bottom: the temperature dependence of the soft mode at \vec{q}_R (from Ref. 8).
- Fig. 6. Inelastic spectra of SrTiO_3 near the phase transition temperature. The left hand side shows the soft mode behavior of the phonon; the right hand side shows the divergence of the central peak (from Ref. 12).
- Fig. 7. Integrated central-peak intensity of hydrogen-reduced SrTiO_3 as a function of $(T - T_c)$ for different carrier concentration (from Rev. 19).

- Fig. 8. Temperature dependence of TA modes propagating along $\vec{q} = (\zeta, \zeta, 0)$ $2\pi/a$ polarized along $[1\bar{1}0]$ for Nb_3Sn . $2\pi/a = 1.19 \text{ \AA}^{-1}$ at 46 K. (from Ref. 21).
- Fig. 9. Spectra of $[\zeta\zeta0]$ shear mode of Nb_3Sn with $\zeta = 0.02$ measured at $(2-\zeta, 1+\zeta, 0)$ (from Ref. 21).
- Fig. 10. Stacking of the atomic planes along the $[111]$ direction and the motion necessary to take fcc ABC ABC stacking into a hcp AB AB AB stacking. The two waves are 180° out of phase. (from Ref. 23).
- Fig. 11. The temperature dependence of the satellites observed in single crystals of $Ti_{50}Ni_{47}Fe_3$. The vertical line corresponds to the commensurate $(2/3, 1/3, 0)$ position. (from Ref. 27).
- Fig. 12. The temperature dependence of the (100), (110), and (111) Bragg peaks in polycrystalline $Ti_{50}Ni_{47}Fe_3$. The splitting of the (110) and (111), and no splitting of the (100) suggest a rhombohedral distortion. (from Ref. 27).

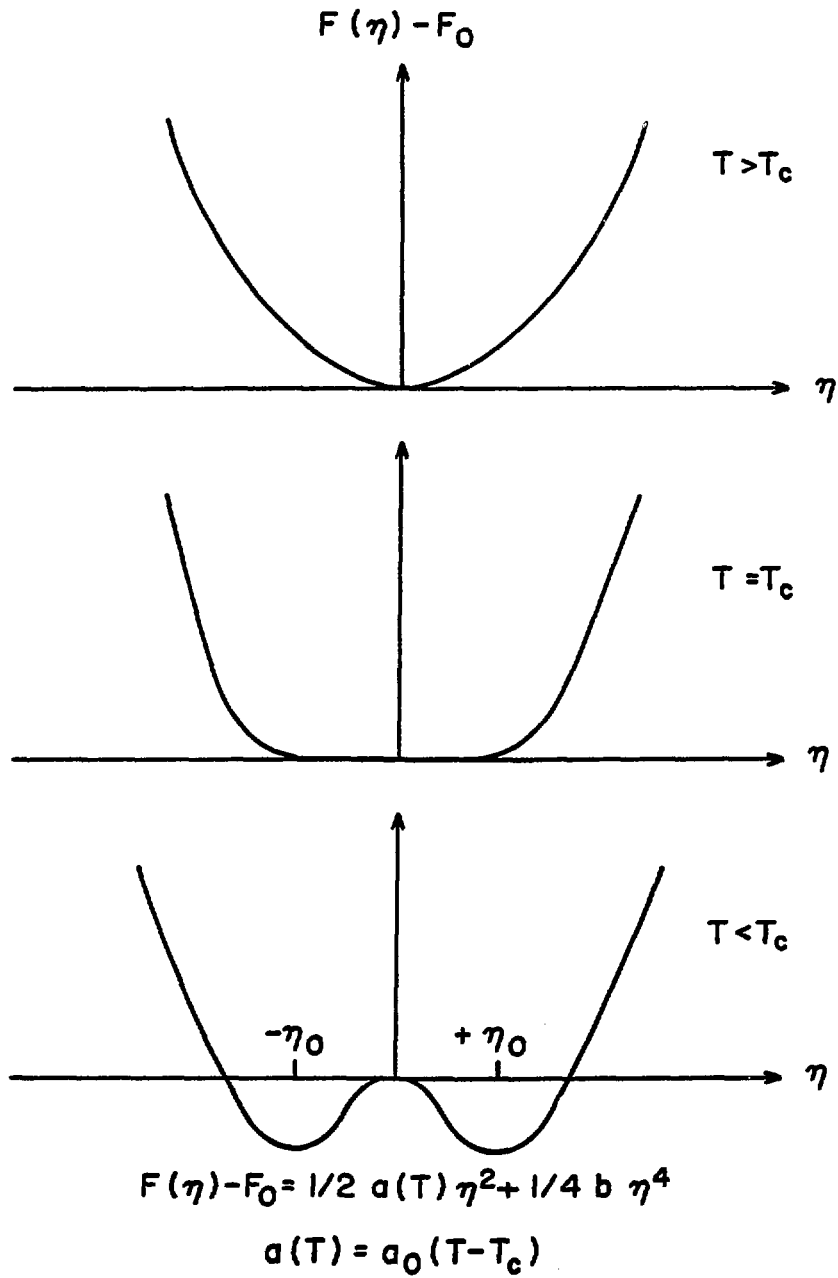


FIGURE 1

H-7 TRIPLE AXIS SPECTROMETER

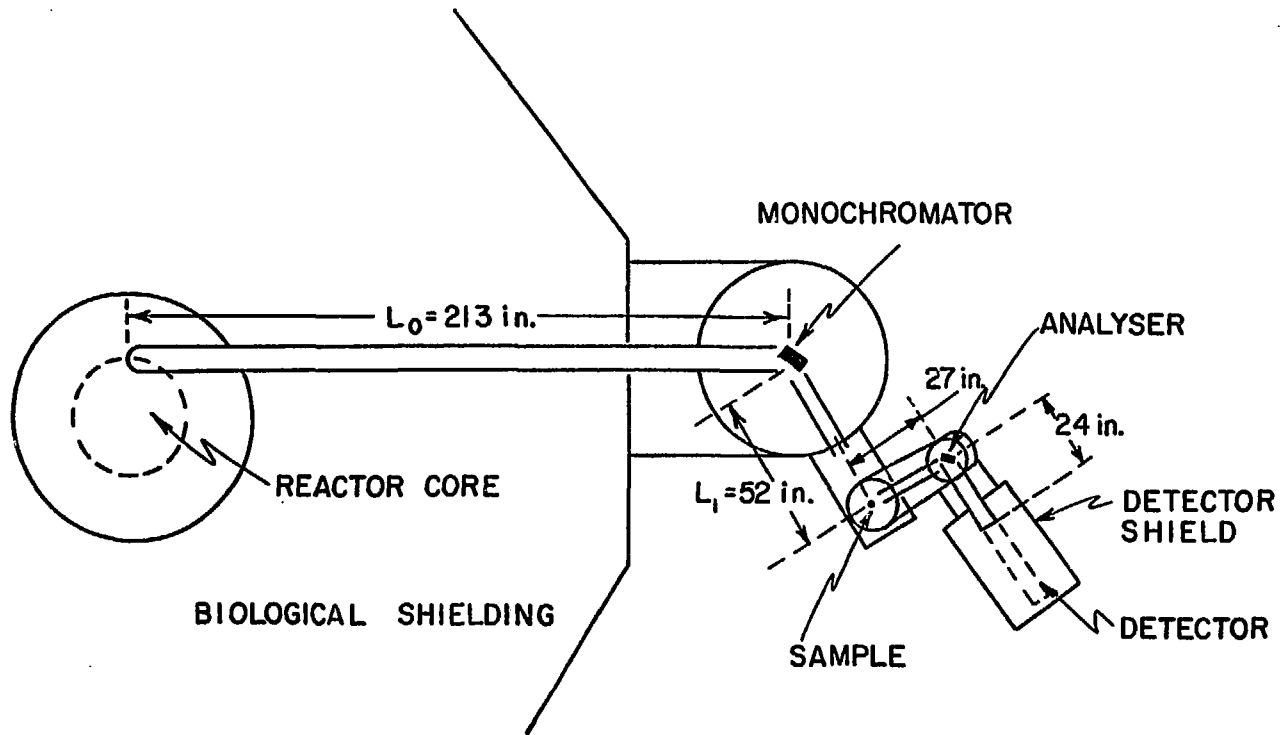


FIGURE 2

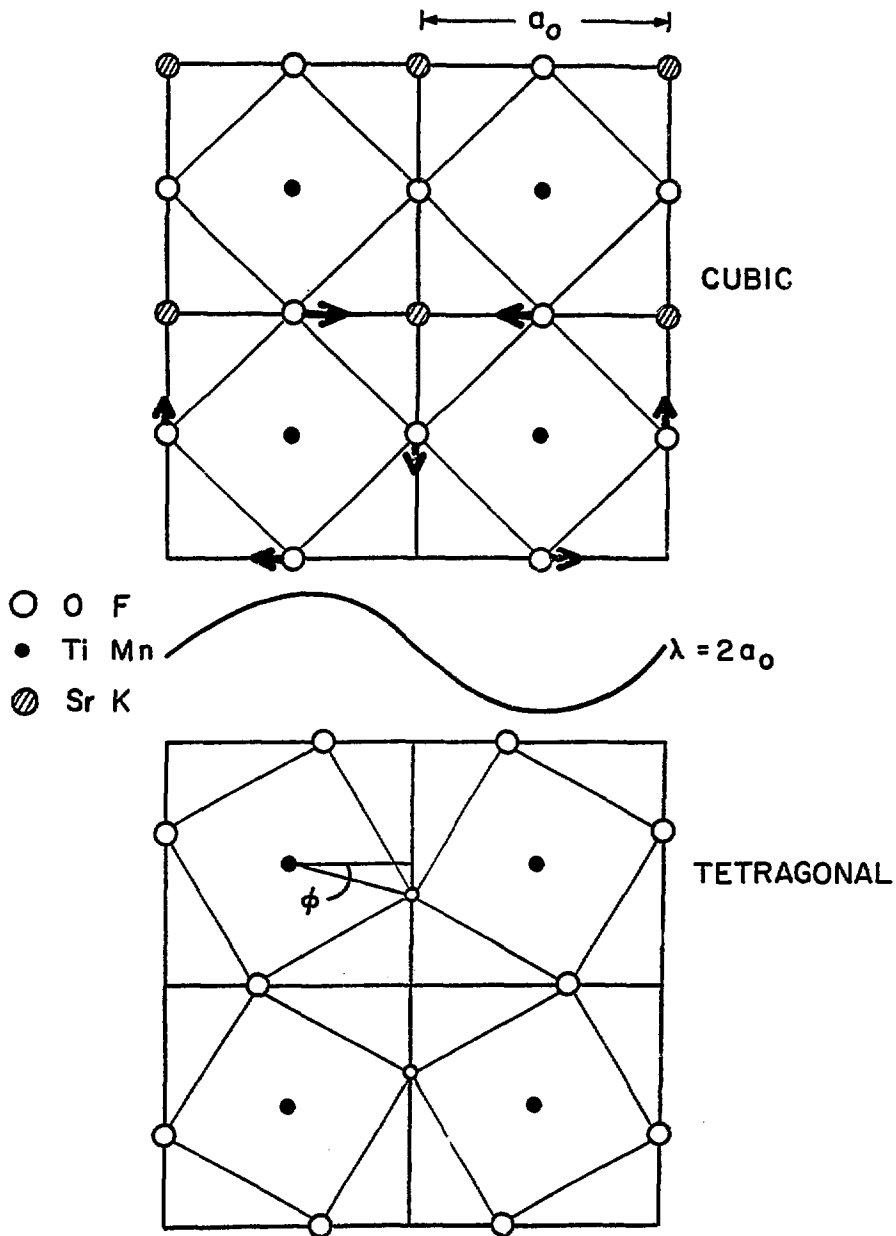


FIGURE 3

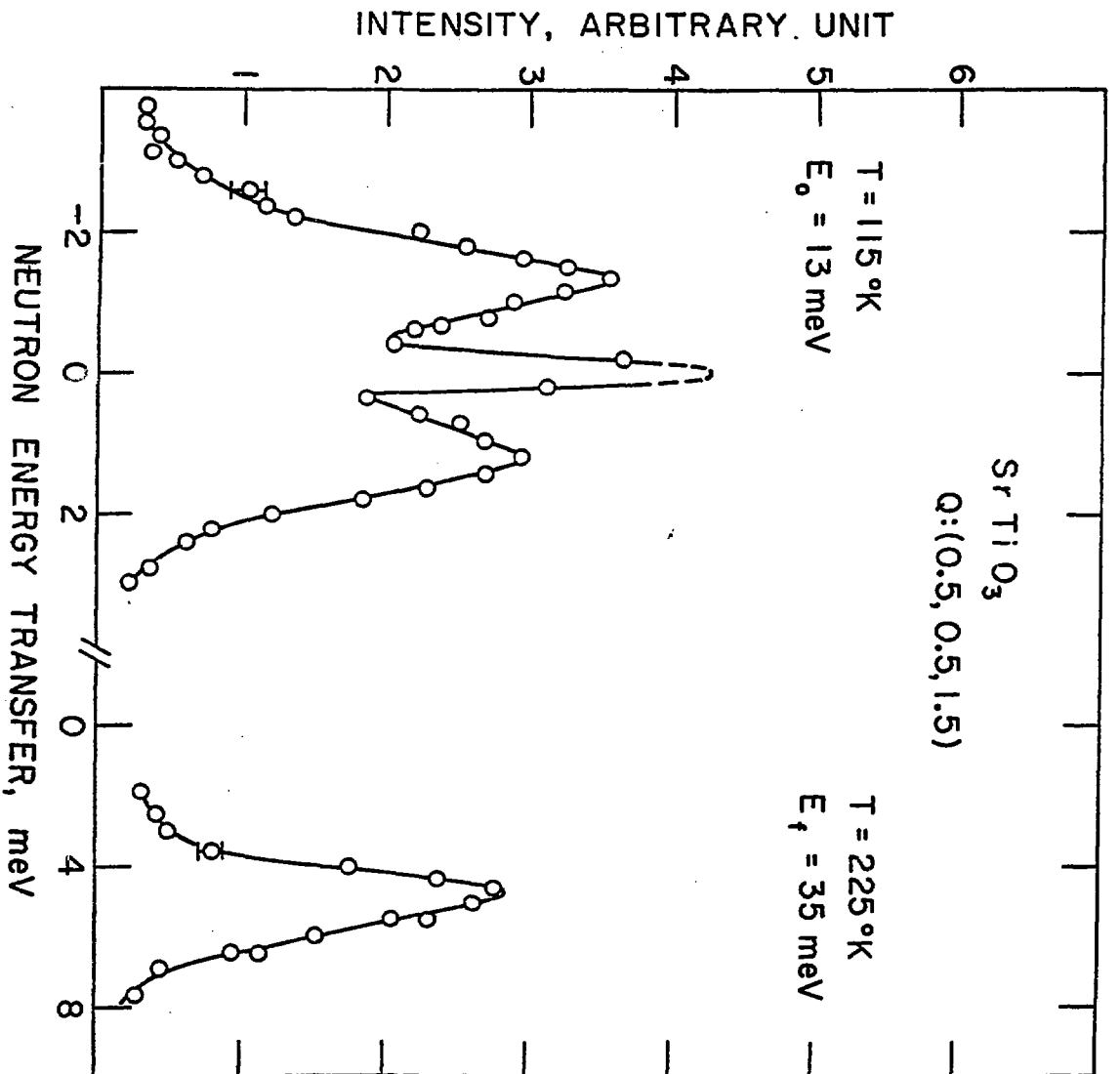


FIGURE 4

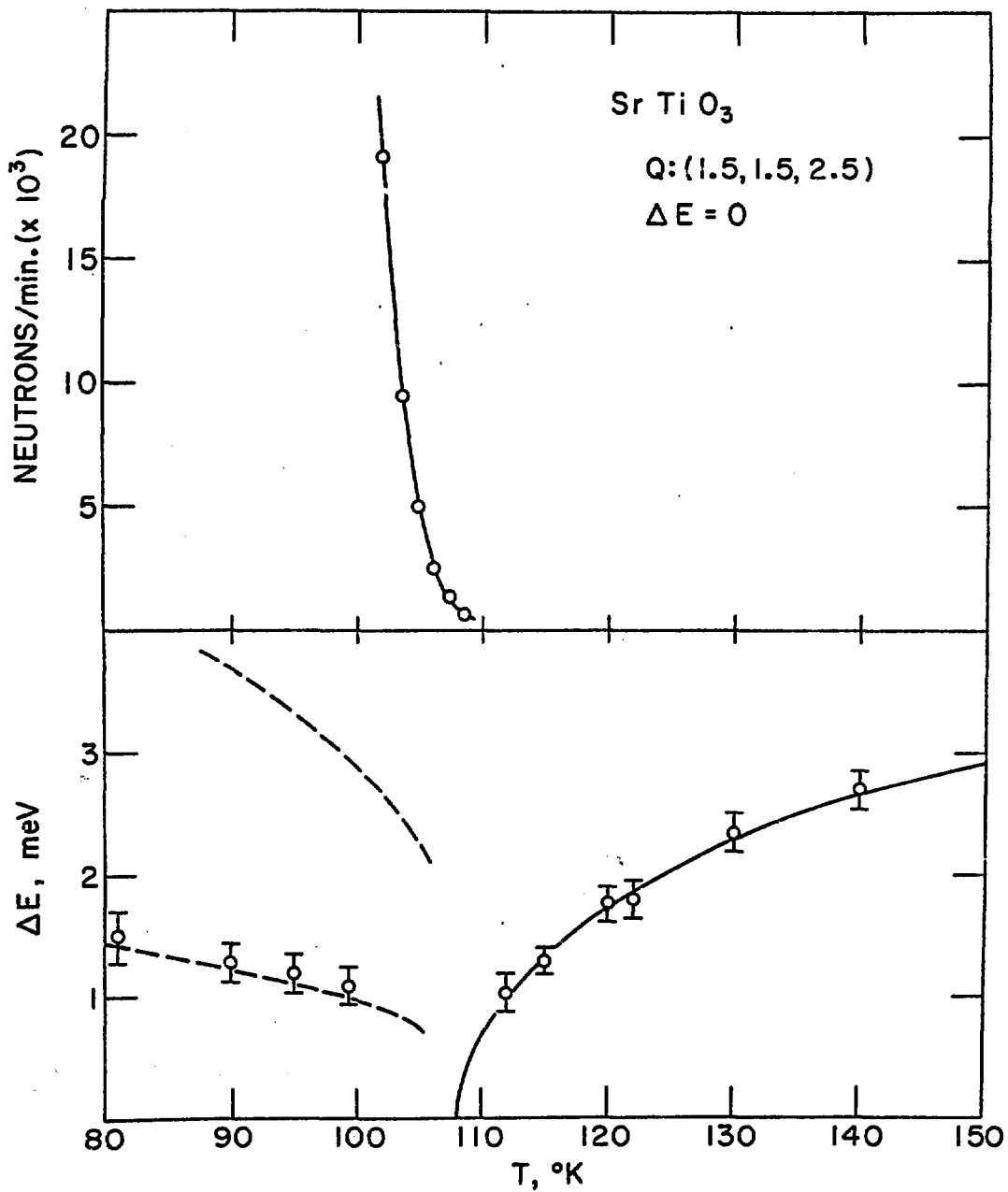


FIGURE 5

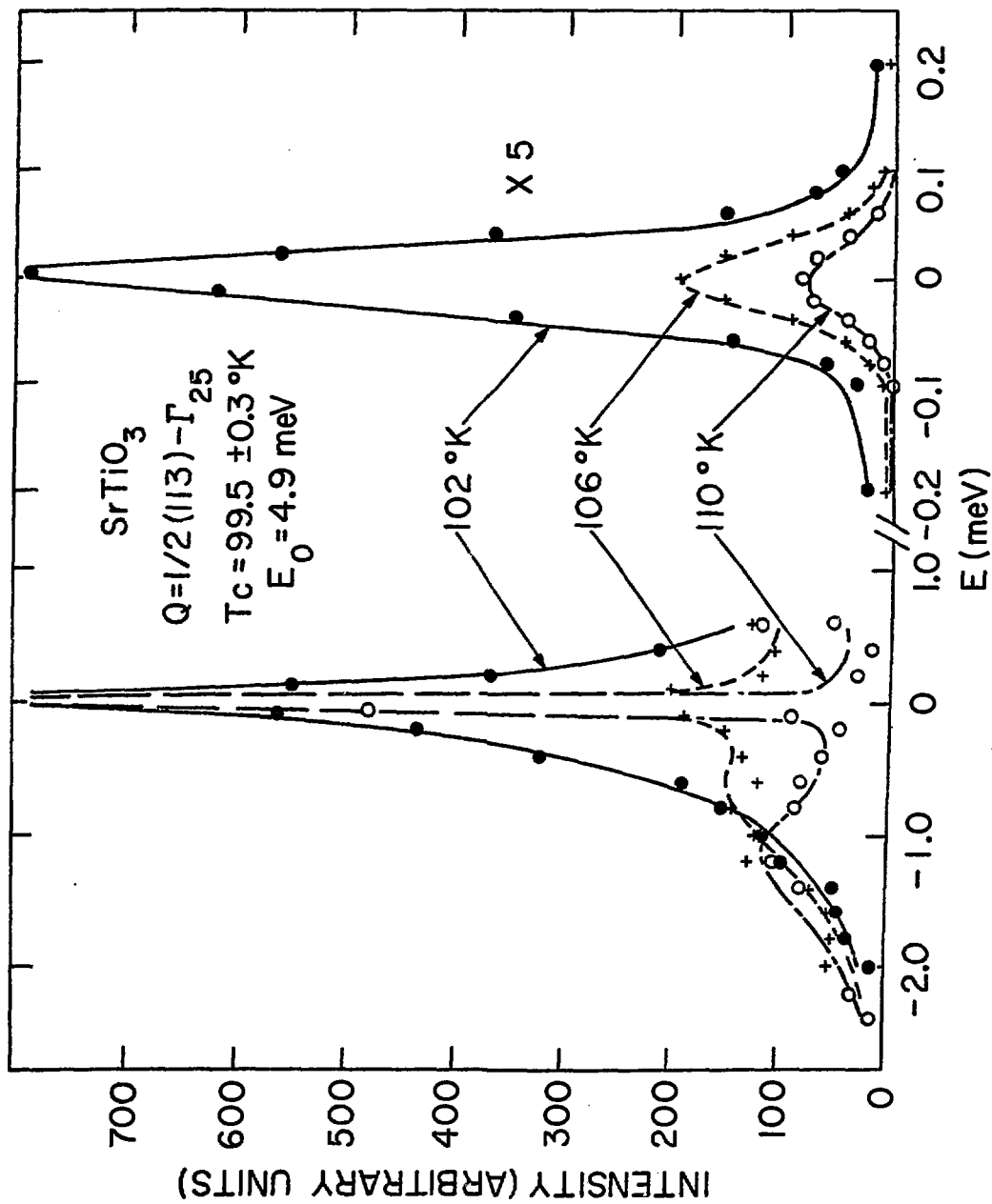


FIGURE 6

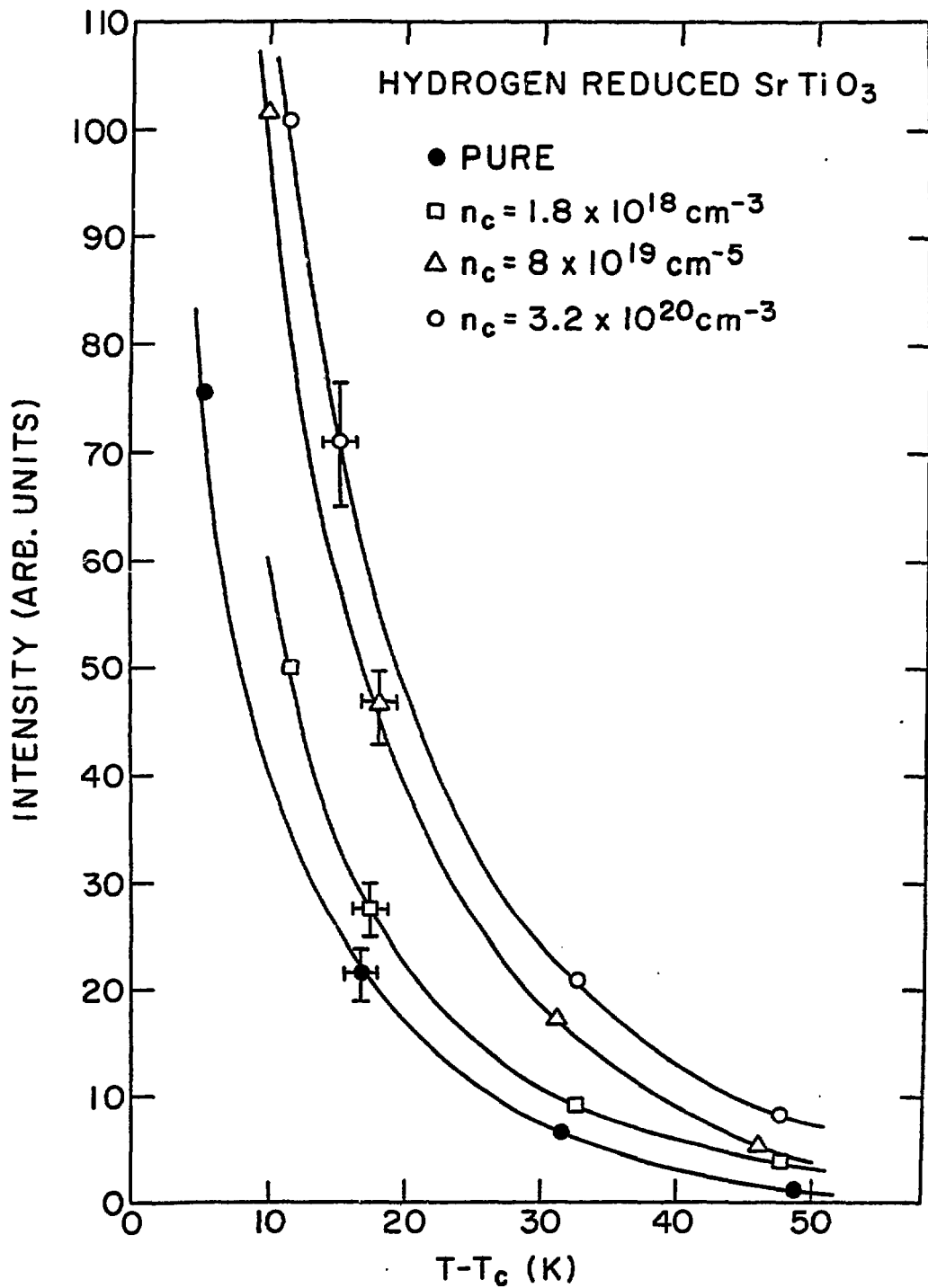


FIGURE 7

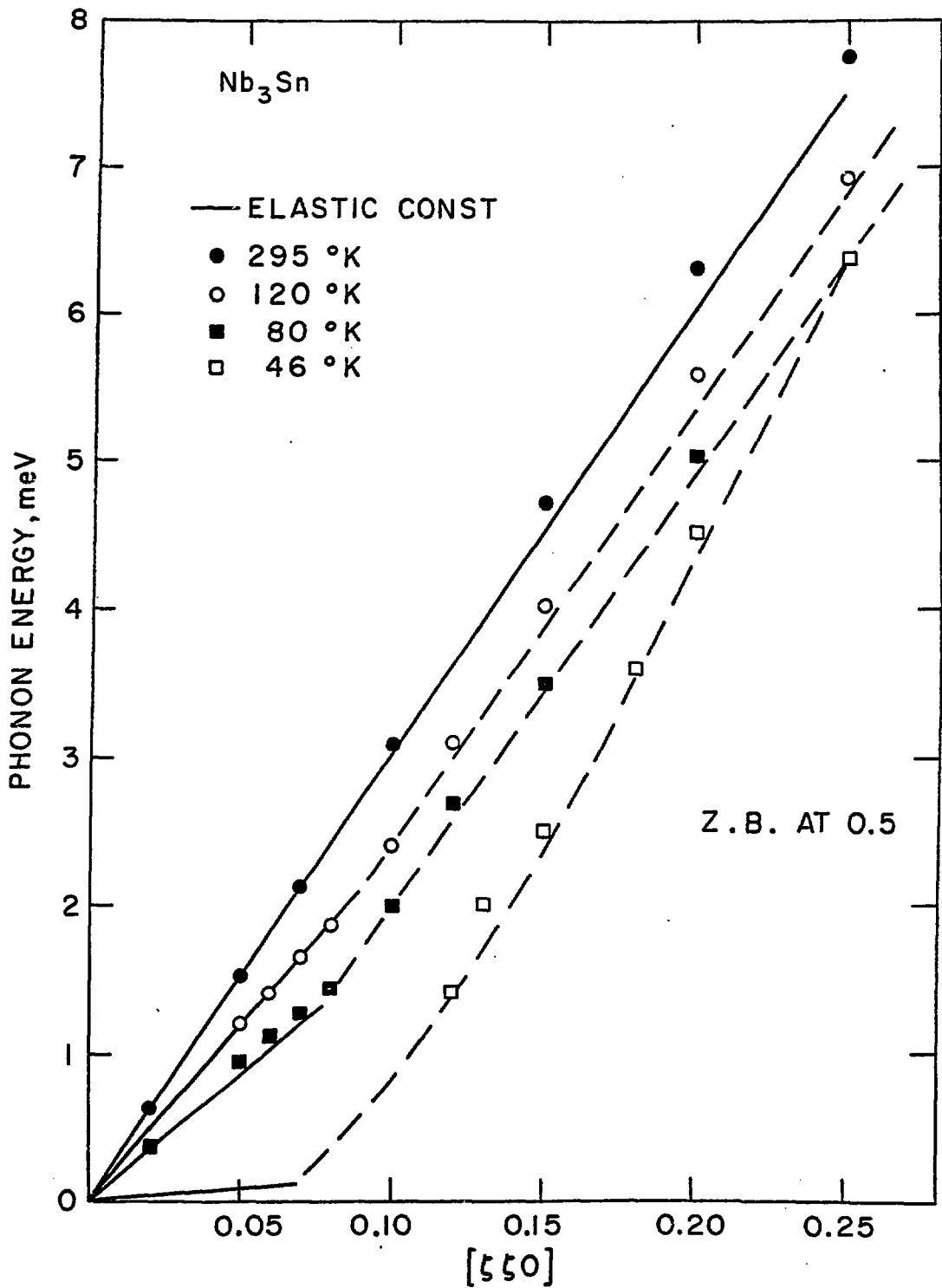


FIGURE 8

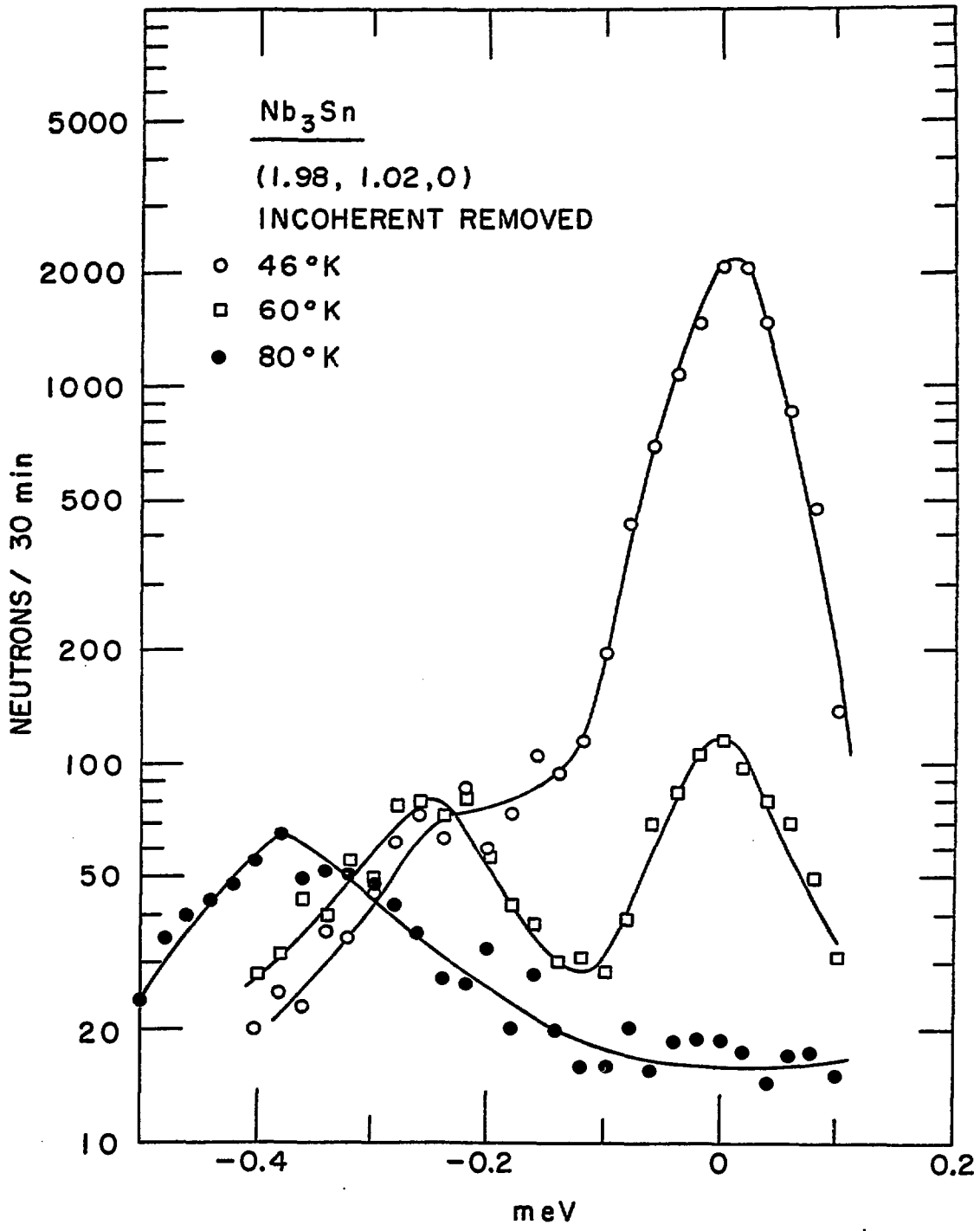
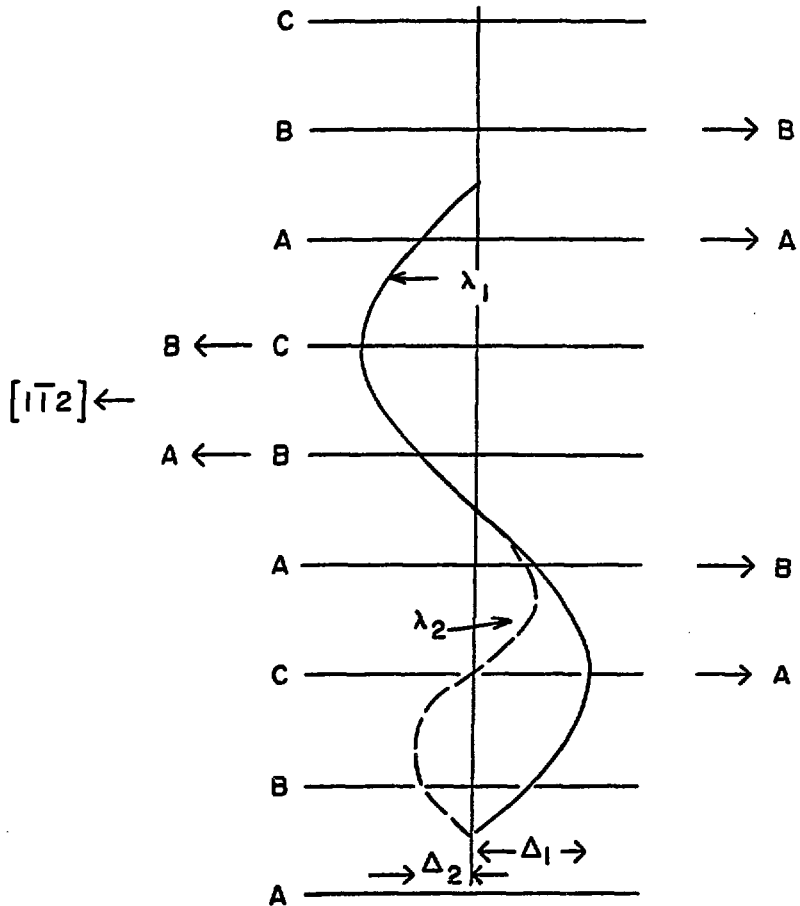


FIGURE 9

8-128-71

FCC \rightarrow HCP

$[111]$



$$\lambda_1 = 6d_{[111]}$$

$$\lambda_2 = 1/2 \lambda_1$$

$$\vec{q}_1 = 1/6 (1, 1, 1)$$

$$\vec{q}_2 = 1/3 (1, 1, 1)$$

$$\Delta_2 = 1/\sqrt{3} \Delta_1$$

FIGURE 10

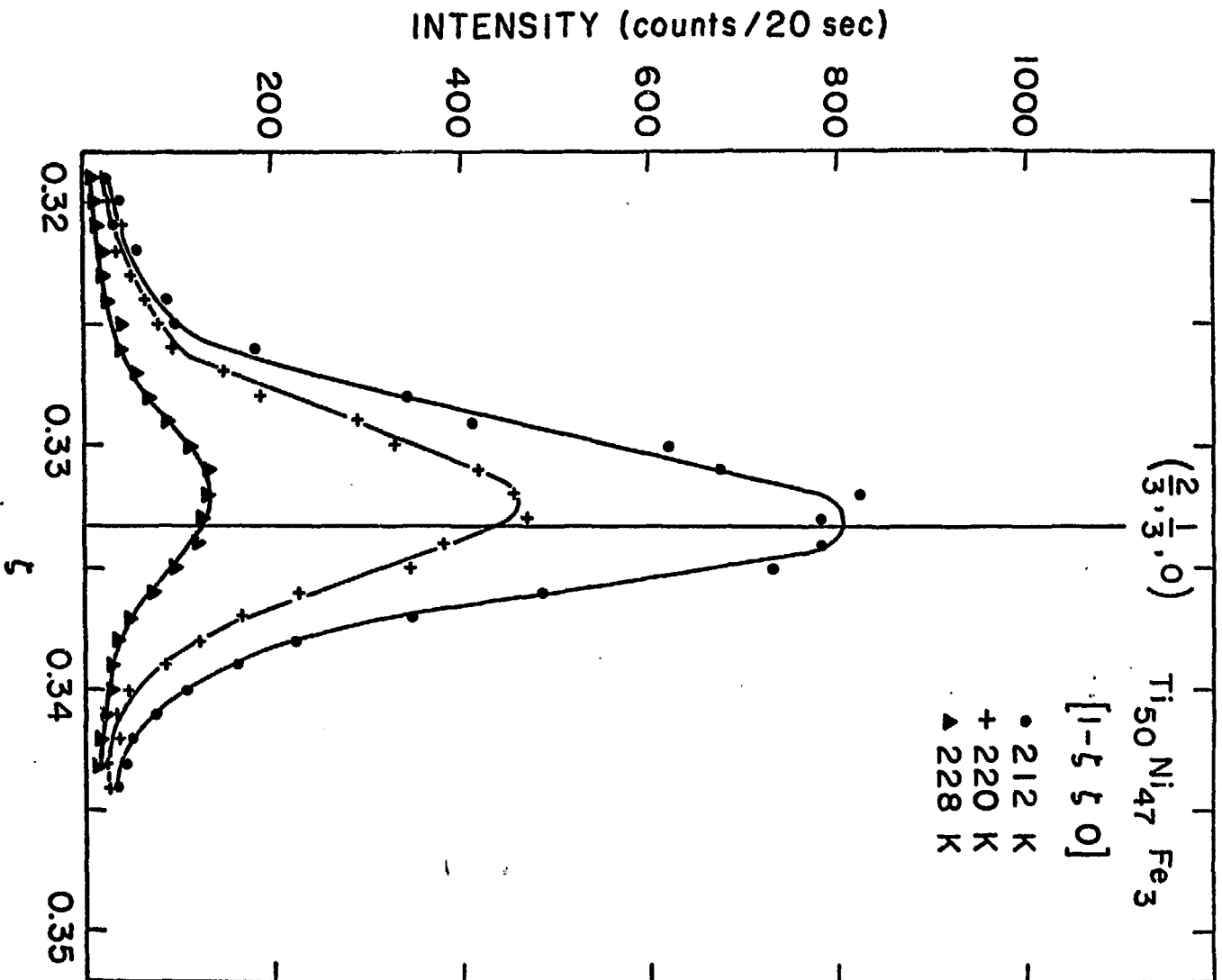


FIGURE 11

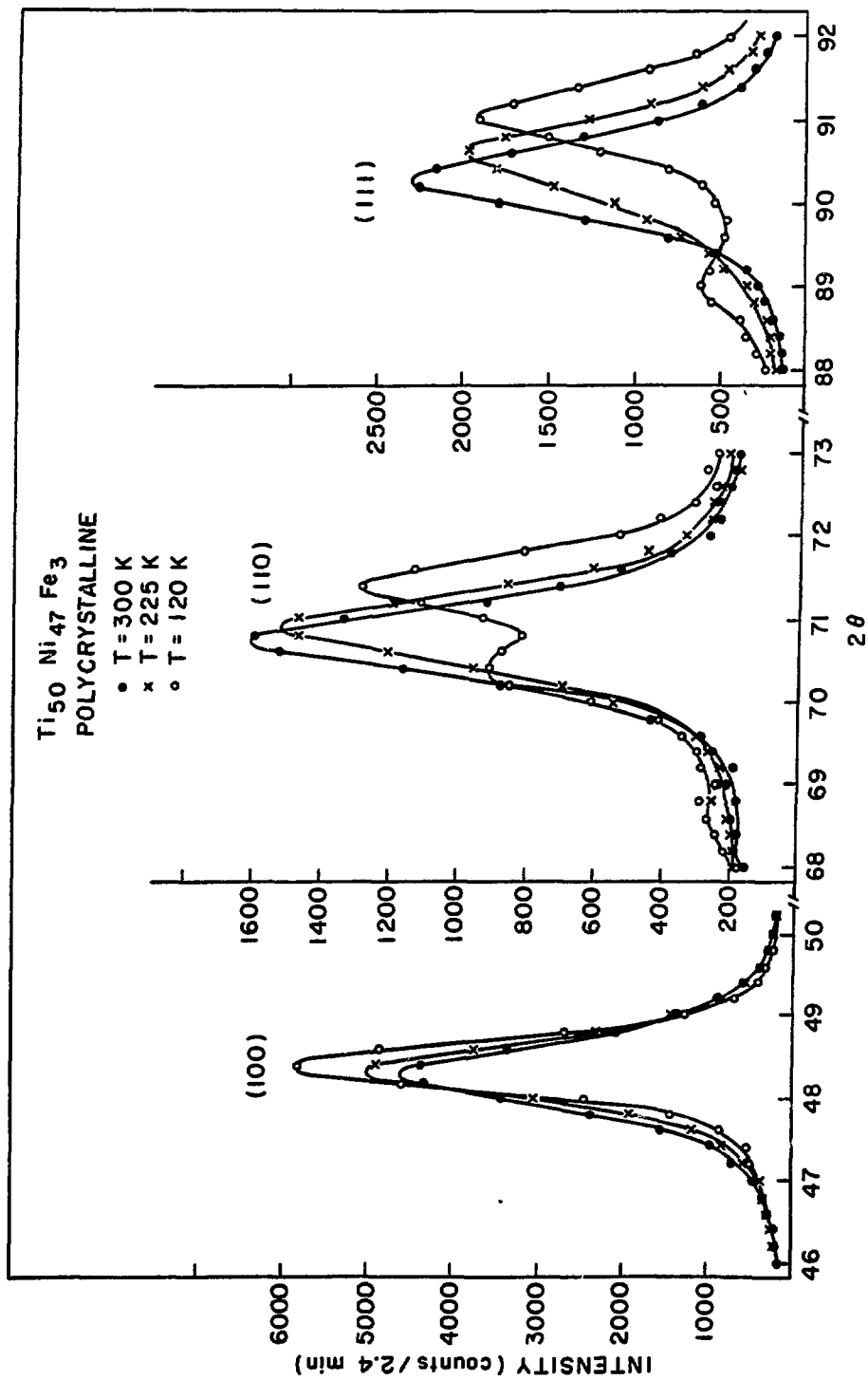


FIGURE 12